9th AUSTRALASIAN
FLUID MECHANICS CONFERENCE
AUCKLAND, 8-12 DECEMBER 1986

Flow in a Rotating Sliced Cylinder: A Comparison of Laboratory and Numerical Models

A. BECKER

Department of Mathematics, Monash University, Clayton, Victoria, Australia.

ABSTRACT

The rotating sliced cylinder is considered as a simple model of the wind-driven ocean circulation. The model consists of a rotating right-cylinder with the base inclined at a small angle, containing a homogeneous fluid. The interior flow is driven by the cylinder lid which rotates steadily at a slightly different rate to the rest of the container. For critical values of the flow parameters $\lambda \alpha Ro/E^{\frac{1}{2}}$ and the bottom slope α, the flow becomes unstable. By comparing the results of numerical models for the inviscid and viscous flows with laboratory experiments it is shown that a possible mechanism for this unsteadiness is a free shear layer instability.

INTRODUCTION

The rotating sliced cylinder is illustrated in Figure 1. It consists of a cylindrical basin of radius l^* and average depth d^*, filled with a homogeneous fluid, rotating at a uniform angular velocity Ω^*. The lower surface is formed by a plane intersecting the cylinder at a small angle β, while the upper surface is normal to the cylinder axis and rotates steadily with excess angular velocity $\varepsilon\Omega^*$.

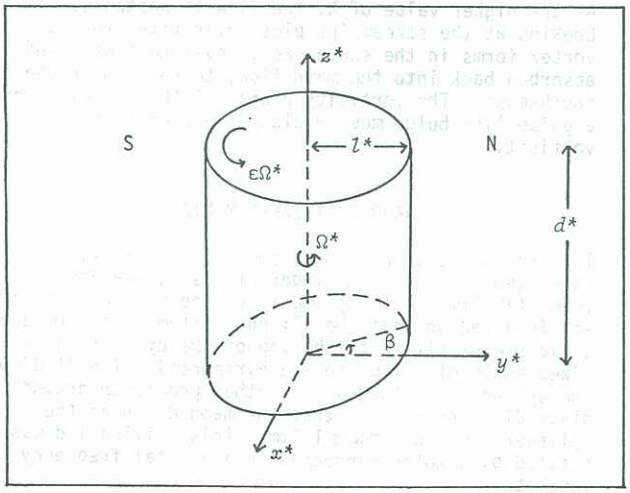

Figure 1: The rotating sliced cylinder model.

The sliced cylinder was first studied as a model of the large scale ocean circulation in mid-latitudes. In this analogy, the cylinder represents the ocean basin and the rotating lid simulates the surface wind stress. The sloping base of the cylinder models the so-called "β-effect" i.e. the effect of the variation of the earth's rotation with latitude.

Pedlosky and Greenspan (1967) introduced the sliced cylinder model and studied the linearised equations for the inviscid flow. Beardsley (1969) also studied the linear equations and carried out some laboratory experiments noting that the flow became unsteady for large values of the driving stress. Beardsley (1973) and Beardsley and Robbins (1975) compared a numerical model of the viscous flow to the experimental results and concluded that the observed unsteadiness was due to a Rossby wave instability.

In this paper, numerical models for the inviscid and viscous flows are compared to the results of laboratory experiments and an attempt is made to explain the unsteadiness of the flow in terms of a shear layer instability.

FORMULATION

The flows considered are those of an incompressible fluid of constant density and kinematic viscosity ν^*, the Ekman and Rossby numbers are defined in the usual way:

$$E = \frac{\nu^*}{\Omega^* l^{*2}} \ll 1 \quad \text{and} \quad Ro = \frac{U^*}{\Omega^* l^*} = O(E^{\frac{1}{2}}) \qquad (1)$$

where U^* is a typical velocity scale $U^*=\varepsilon l^*\Omega^*$. The Navier-Stokes equation in terms of these variables are

$$\frac{\partial \underset{\sim}{u}^*}{\partial t^*} + (\underset{\sim}{u}^*.\nabla)\underset{\sim}{u}^* + 2\underset{\sim}{\Omega}^* \times \underset{\sim}{u}^* = \frac{1}{\rho^*}\nabla^* P^* + \nu^*\nabla^{*2}\underset{\sim}{u}^* \qquad (2)$$

$$\nabla^*.\underset{\sim}{u}^* = 0 \qquad (3)$$

where $\underset{\sim}{u}^*$ is the fluid velocity relative to the rotating frame and P^* is the reduced pressure, i.e. with the centrigugal contribution subtracted. Equations (2) and (3) are scaled by the length scale l^*, velocity scale U^* and time scale $(\Omega^*)^{-1}$ and expanded in powers of $E^{\frac{1}{2}}$. The resulting non-dimensional equations for the flow to lowest order are

$$\frac{\partial \zeta}{\partial t} + \lambda(\underset{\sim}{u}.\nabla)\zeta = 1 - \zeta - \alpha v + \delta^2\nabla^2\zeta \qquad (4)$$

$$\nabla^2\psi = \zeta \qquad (5)$$

where $\underset{\sim}{u}=(u,v,0)$, $\zeta=\hat{k}.(\nabla\times\underset{\sim}{u})$, and $\delta=(dE^{\frac{1}{2}}/2)^{\frac{1}{2}}$. The streamfunction ψ can be defined in the usual way, since the flow is geostrophic and hence two-dimensional to this order.

The two key $O(1)$ flow parameters are

$$\lambda = \frac{Ro\ d}{2E^{\frac{1}{2}}} \quad \text{and} \quad \alpha = \frac{\tan\beta}{E^{\frac{1}{2}}} \qquad (6)$$

where α is the bottom slope scaled by the Ekman layer thickness and λ is the scaled Rossby number and is related to the magnitude of the driving stress.

INVISCID MODEL

For the inviscid flow in the sliced cylinder, the governing equations are (4) and (5) omitting the last term in (4) which is $O(E^{\frac{1}{4}})$. These equations were solved on a uniform polar grid using second order central differences for the r and θ derivatives.

The vorticity equation (4) was solved for ζ using an "alternating directions implicit" method and the Poisson equation (5) was then solved for the stream-function ψ using Fourier transforms. The equations are thus alternately integrated forward in time to steady state.

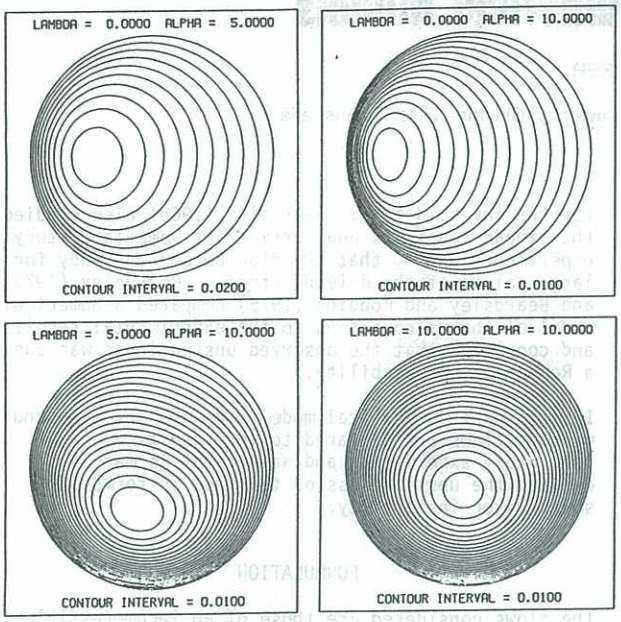

Figure 2: Streamfunction plots for the inviscid model.

A selection of results from this numerical model are shown in Figure 2. With λ=0, the plots show the effect of varying α (or the bottom slope of the cylinder) and we see that the flow pattern is asymmetric, the central vortex having moved to the "western" side of the cylinder, forming a strong western boundary current of thickness $1/\alpha$. The flow is still symmetric about the y-axis, however, increasing λ (i.e. increasing the effect of the driving stress) causes the main vortex to be displaced toward the south so that the flow pattern loses its symmetry altogether. For larger λ, the vortex is displaced further south until the flow becomes almost symmetric about the x-axis. There is no evidence of unsteadiness in these flows.

VISCOUS MODEL

To study the viscous flow, we solve equations (4) and (5) retaining the side wall friction term which was omitted from the inviscid model. These equations were solved numerically on a stretched polar grid using a similar method to that described in the previous section. For details of this model see Becker and Page (1986).

In Figure 3 flows resulting from this viscous model are compared to the inviscid flows. Again, there is no sign of unsteadiness in the inviscid flows. The viscous flows, while similar in character to the inviscid flows, show a slower region of flow in the eastern half of the cylinder. For the higher value of λ, a small sub-vortex has formed in the north. The corresponding vorticity plots show a region of strong vorticity in the centre of the cylinder. This represents the separated sidewall boundary layer which has moved into the interior flow region causing the disturbance to the streamlines in the eastern half of the cylinder.

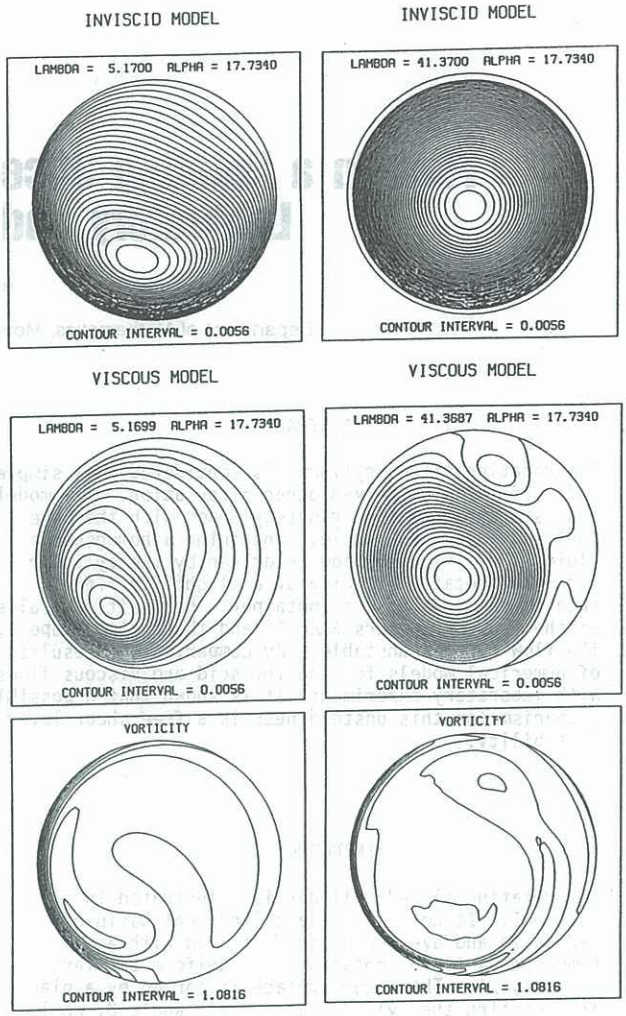

Figure 3: Comparison of inviscid and viscous flow models.

At the higher value of λ, the flow is unstable. Looking at the streamline plots over time, the sub-vortex forms in the south-east, moves northward and is absorbed back into the main flow, to re-form in the south-east. The vorticity plots for this λ value show a pulse-like bulge moving along the region of high vorticity.

LABORATORY EXPERIMENTS

The experimental apparatus, shown in Figure 4, consisted of a glass cylinder of inside diameter 150mm (±0.01mm). The geometry of the sliced cylinder was inverted so that the sliced "bottom" was formed by a glass disk fitted to the top of the cylinder at a fixed angle of β=7.5° to the horizontal. The "lid" of the cylinder was formed by another precision ground glass disk inserted so that the mean depth of the cylinder thus formed was 175mm. This driving lid was rotated by a motor connected to a digital frequency generator.

The cylinder was mounted on a turntable 1m in diameter which was rotated by a driving motor controlled by a feedback loop from the table. The turntable could be rotated at speeds varying from 5-100rpm.

Flow visualisation was achieved using a suspension of highly reflective "mearle" flakes (titanium dioxide coated mica flakes) illuminated from the side. A camera with remote shutter control was mounted above the cylinder and a video camera was used to view the flow while the cylinder was rotating. When the flow appeared to be steady, a series of photographs was taken to ensure repeatability of the flow pattern.

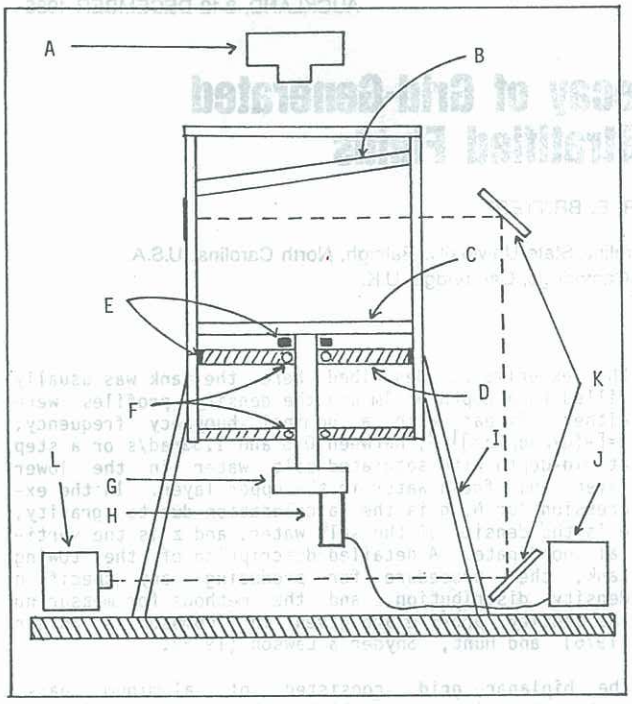

Figure 4: A: 35mm camera; B: sloping "bottom"; C: rotating glass disk; D: perspex disk; E: seals; F: bearings; G: driving gear; H: driving motor; I: support; J: digital frequency generator; K: mirrors; L: light source.

In Figure 5, steak photographs are shown for α and λ values matching those of Figure 3. For the lower value of λ, the main vortex is clearly present in the south-west and the flow is almost stagnant elsewhere. With λ=41.37, the main vortex has increased in size and a sub-vortex appears in the north. In fact, this sub-vortex is periodically formed in the south-east, and moves northward, matching very closely, the behaviour of the numerical model for the viscous flow for the corresponding parameter values.

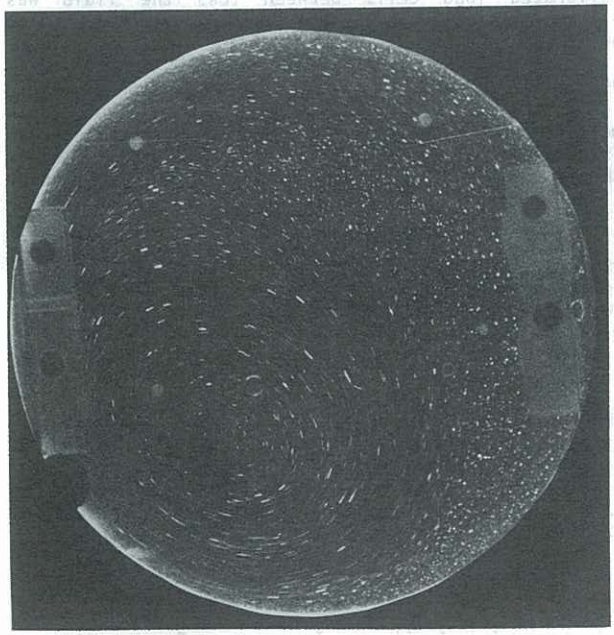

Figure 5a: Streak photograph for α=17.34 and λ=5.17.

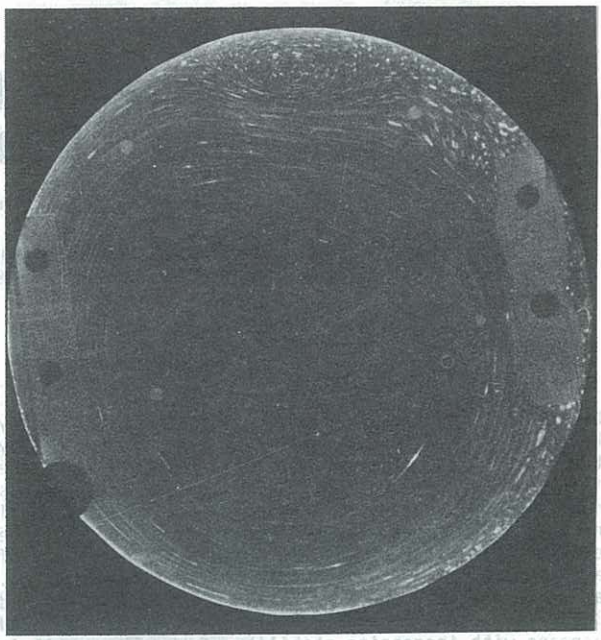

Figure 5b: Streak photograph for α=17.34 and λ=41.37.

CONCLUSION

The inviscid flow is stable over a large range of values of α and λ (which is inconsistent with Beardsley and Robbins who expected a Rossby wave instability). For large values of the driving stress, both the numerical model for the viscous flow and the laboratory flows become unstable. This implies that the instability is due to viscous effects and since the flow does separate, the unsteadiness is most likely due to a shear layer instability.

REFERENCES

Beardsley, R C (1969): A laboratory model of the wind-driven ocean circulation. J. Fluid Mech., vol. 38, 255-271.

Beardsley, R C (1973): Numerical Methods of Ocean circulation. NAS Symposium Proceedings, 311-326.

Beardsley, R C; Robbins, K (1975): The "sliced cylinder" laboratory model of the wind-driven ocean circulation. Part I: steady forcing and topographic Rossby wave instability. J. Fluid Mech., vol. 69, 27-40.

Becker, A; Page, M A (1986): Flow separation and unsteadiness in a rotating sliced cylinder. To be submitted to Geophys. Astrophys. Fluid Dynamics.

Pedlosky, J; Greenspan, H P (1967): A simple laboratory model for the oceanic circulation. J. Fluid Mech., vol. 27, 291-304.